Two-sections tapered diode lasers for 1 Gbps free-space optical communications with high modulation efficiency

N. Michel , M. Ruiz , M. Calligaro[a], Y. Robert[a], M. Lecomte[a], O. Parillaud[a], M. Krakowski[a**], I. Esquivias[b], H. Odriozola[b], J.M. G. Tijero[b], C.H. Kwok[c], R.V. Penty[c], I.H. White[c]

[a]Alcatel-Thales III-V Lab, Route Départementale 128, 91767 Palaiseau, France
[b]Universidad Politécnica de Madrid, ETSI Telecomunicación, Madrid 28040, Spain
[c]Center for Photonic Systems, Electrical Engineering Division, Department of Engineering, University of Cambridge, 9 JJ Thomson Avenue, Cambridge CB3 0FA, United Kingdom

ABSTRACT

High-power (more than 500 mW) and high-speed (more than 1 Gbps) tapered lasers at 1060 nm are required in free-space optical communications and (at lower frequencies of around 100 MHz) display applications for frequency doubling to the green. On a 4 mm-long tapered laser, we have obtained an open eye diagram at 700 Mbps, together with a high extinction ratio of 19 dB, a high optical modulation amplitude of 1.6 W, and a very high modulation efficiency of 19 W/A. On a 3 mm long tapered laser, we have obtained an open eye diagram at 1 Gbps, together with a high extinction ratio of 11 dB, an optical modulation amplitude of 530 mW, and a high modulation efficiency of 13 W/A.

INTRODUCTION

High-brightness tapered lasers

High brightness diode lasers at 1060 nm are required in free-space optical communications, and also in laser display applications, by frequency doubling to green at 530 nm. In both applications, a high-speed, low-current driver is required for commercial use, which has a bandwidth in the range of 1 GHz and a maximum current in the range of 100 mA.

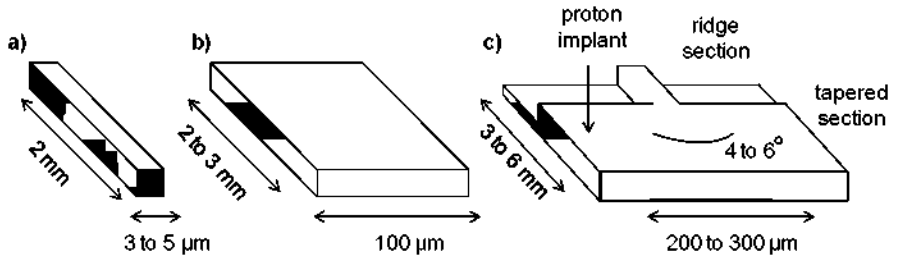

Figure 1: a) single spatial mode laser, b) broad area laser, c) gain-guided tapered laser

On the one hand, single spatial mode, ridge waveguide lasers (Figure 1a) deliver a limited optical power of 1 to 2 W [1], because of their narrow stripe width, which makes heat removal difficult. On the other hand, broad area lasers (Figure 1b) deliver high power [2], but have a highly multimode beam, which is a limitation for coupling into optical fibers. Tapered lasers [3] (Figure 1c) combine both high power and good beam quality: they contain a ridge waveguide section, which acts as a modal filter, and a tapered section of increasing width, which delivers both high power and good beam quality.

* nicolas.michel@3-5lab.fr; phone +33 (0)1 69 41 58 26; www.3-5lab.fr
** michel.krakowski@3-5lab.fr; phone +33 (0)1 69 41 58 25

Single section and two-sections tapered lasers

In both free-space (~ 1 Gbps) optical communications and display applications (~ 100 Mbps), a high-speed, low-current driver is required for commercial use, which has a maximum current in the range of 100 mA. In tapered lasers, the ridge and tapered sections may have either a common electrical contact (Figure 2), or either 2 separate electrical contacts (Figure 3).

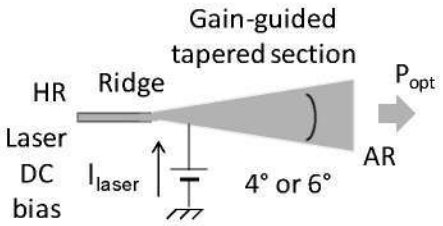

Figure 2: single section tapered laser

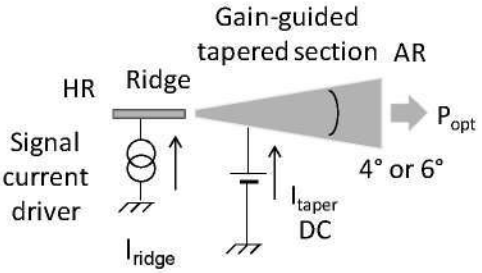

Figure 3: two-sections tapered laser

On single contact lasers (Figure 2), the external differential efficiency $\Delta P_{opt}/\Delta I_{laser}$ is the ratio of the emitted output power P_{opt} versus the injected current I_{laser} above threshold. This value $\Delta P_{opt}/\Delta I_{laser}$ is limited by the physical law[1] in (EQ 1):

$$\frac{\Delta P_{Opt}}{\Delta I_{laser}} \leq \frac{hc}{\lambda} = \frac{1.24}{1.06} = 1.16\ W/A \qquad \text{(EQ 1)}$$

The above maximum value of 1.16 W/A is valid at λ = 1.06 µm. In the applications where an output power of 1 W or more is needed, the required driving current of more than 1 A is not compatible with low-cost commercial drivers. On two-sections tapered lasers (Figure 3), the variable signal current I_{ridge} is applied only to the ridge, while the tapered section is kept constant at a high DC bias I_{taper}. Under this configuration, the key advantage is the high modulation efficiency (ME), which is given by (EQ 2):

$$ME = \frac{\Delta P_{Opt}}{\Delta I_{ridge}} \qquad \text{(EQ 2)}$$

Under this configuration, a very high modulation efficiency of 50 W/A was already demonstrated in the static regime [4], which is well above the allowed maximum of 1.16 W/A for single section lasers. The ME of 50 W/A on two-section lasers is significantly higher than previously reported values for increasing the modulation efficiency, such as the stacking of multiple diode lasers, or bipolar cascade lasers with Esaki junctions [5]. Moreover, an error-free [6], Bit-Error-Rate (BER) of less than 10^{-9} was reported on two-sections tapered lasers at 700 Mbps. In this paper, we will present two sections lasers based on the following plan:

- I- Laser structure
- II- Simulations
- III- Tapered lasers in the static regime
- IV- Beam properties in the static regime
- V- Operation in the dynamic regime

[1] *In (EQ1), h is Planck's constant, c the speed of light, and λ the optical wavelength in µm. (EQ1) means that each injected pair of carriers in the laser generates no more than one output photon, which is true for single electrode interband lasers. The formula does not hold when several lasers are connected in series or in the case of bipolar cascade lasers with integrated Esaki junctions.*

I- LASER STUCTURE

The 1060 nm symmetric Al-free active region structure (Figure 4) contains two barriers made of GaInAsP and one GaInAs quantum well, which are between two AlGaAs claddings. On this structure, we have realised broad-area lasers with length of either 1 or 2 mm and 100 µm width. The lasers were mounted down with indium solder on copper submounts. On the 2 mm x 100 µm laser (Figure 5), we have obtained a high power of 3 W per facet, together with a high maximum wall-plug efficiency of 66%.

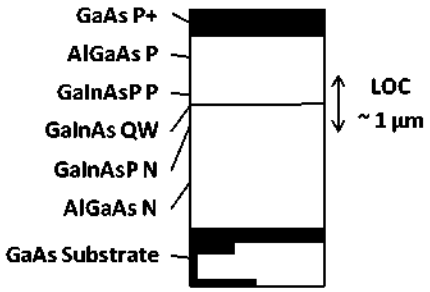

Figure 4: symmetric Al-free active region structure

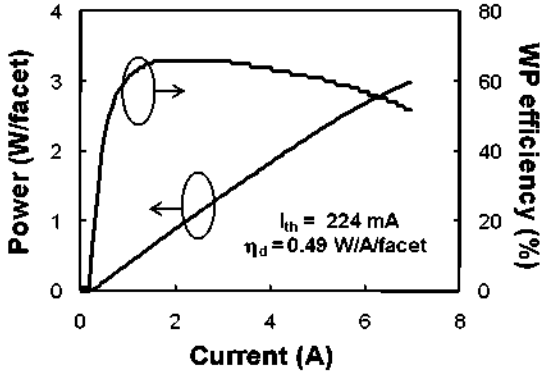

Figure 5: power characteristics
(2 mm x 100 µm laser, 20°C CW)

Based on the measurements on broad area lasers, we have extracted the internal parameters of the semiconductor structure (Figure 6, Figure 7). We have obtained low optical losses of 0.9 cm^{-1}, a high internal quantum efficiency of 98%, a modal gain coefficient of 13.8 cm^{-1}, and a low transparency current density of 64 A/cm^2.

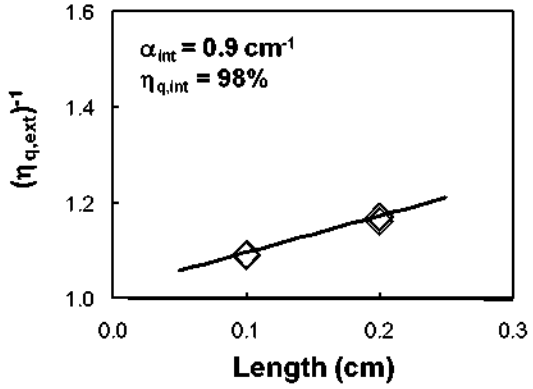

Figure 6: internal losses α_i and internal quantum efficiency η_i

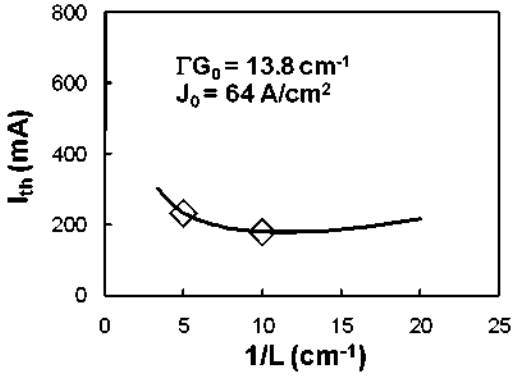

Figure 7: modal gain coefficient ΓG_0 and transparency current density J_0

II- SIMULATION OF TWO-SECTION LASERS

In this section, we have performed simulations in order to achieve the highest modulation efficiency of the two-section tapered lasers. The simulations were based on a quasi-3D code, which includes carrier, optical and thermal effects [7]. In this section, we use a ridge length of 1 mm, a taper length of 2.4 mm, a reflectivity of 95% on the back facet, and a taper angle of 4° [8].

In the first simulation (Figure 8), the front facet reflectivity is of 2.5%. In this case, the output power does not strongly depend on the current I_{ridge} applied to the ridge waveguide, so that the modulation efficiency is poor.

In the second simulation (Figure 9), we have used a front facet reflectivity of 0.1%. In this case, the output power strongly depends on the current I_{ridge}. In particular when I_{ridge} = 0 mA, the laser emission does not occur before I_{taper} = 1.4 A. This means that the modulation efficiency, is high. Based on the simulated power P_{opt} = 0 mW at (I_{ridge} = 0 mA , I_{taper} = 1.4 A) and P_{opt} = 920 mW at (I_{ridge} = 40 mA , I_{taper} = 1.4 A), we find a high modulation efficiency of more than 20 W/A.

$$ME = \frac{\Delta P_{Opt}}{\Delta I_{ridge}} = \frac{920}{40} = 23\ W/A \qquad \text{(EQ 3)}$$

The simulation results presented above can be found in more details in [8].

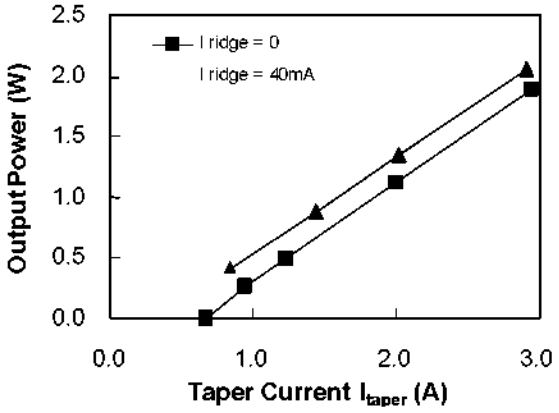

Figure 8: simulation of two-sections tapered laser with 2.5% front-facet reflectivity

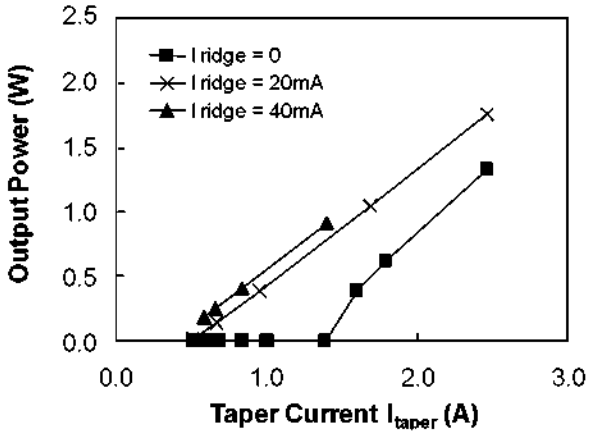

Figure 9: simulation of two-sections tapered laser with 0.1% front-facet reflectivity

III- TWO-SECTION TAPERED LASERS MEASURED IN THE STATIC REGIME

Laser geometries

In this section, we present the power characteristics of two-sections tapered lasers, which are operated under static, CW conditions. We have realised 4 types of lasers, two types with 4 mm length, and two types of 3 mm length. All lasers were mounted epi-side up with indium solder on copper submounts.

Table 1: Summary of laser geometries

Total length (mm)	Front facet reflectivity (%)	Ridge length (mm)	Taper length (mm)	Taper angle (°)
4	0.1	1	3	4
				6
3	2.5	1	2	4
				6

On the 4 mm lasers, the front facet reflectivity is of 0.1%, as suggested by the above simulations in the static regime. On the 3 mm lasers, the tapered section is shorter and the front facet reflectivity is of 2.5%, in order to reduce the BER (Bit Error Rate) under NRZ modulation at 1 Gbps (see last section).

Tapered lasers with 4 mm length

The power characteristics of the 4° lasers are shown in Figure 10 for several values of I_{ridge}. The laser delivers up to 3 W power at 10°C CW (I_{ridge} = 200 mA, I_{taper} = 4 A). However, even with I_{ridge} = 0 mA, lasing occurs when I_{taper} is larger than 1.4 A. For (I_{ridge} = 50 mA, I_{taper} = 1.4 A), the power is of 0.65 W, and for (I_{ridge} = 0 mA, I_{taper} = 1.4 A) the power is of 60 mW so that the modulation efficiency is of :

$$ME = \frac{\Delta P_{Opt}}{\Delta I_{ridge}} = \frac{0.65 - 0.06}{0.05} = 12\ W/A \qquad \text{(EQ 4)}$$

The power characteristics of the 6° lasers are shown in Figure 11 for several values of I_{ridge}. The laser delivers up to 3 W power at 10°C CW (I_{ridge} = 200 mA, I_{taper} = 4A). However, with I_{ridge} = 0 mA, no lasing occurs even when I_{taper} reaches 4 A. The power is of only 90 mW at (I_{ridge} = 0 mA, I_{taper} = 4 A), and reaches 2.6 W at (I_{ridge} = 50 mA, I_{taper} = 4 A). This corresponds to a very high modulation efficiency of 50 W/A:

$$ME = \frac{\Delta P_{Opt}}{\Delta I_{ridge}} = \frac{2.6 - 0.09}{0.05} = 50\ W/A \qquad \text{(EQ 5)}$$

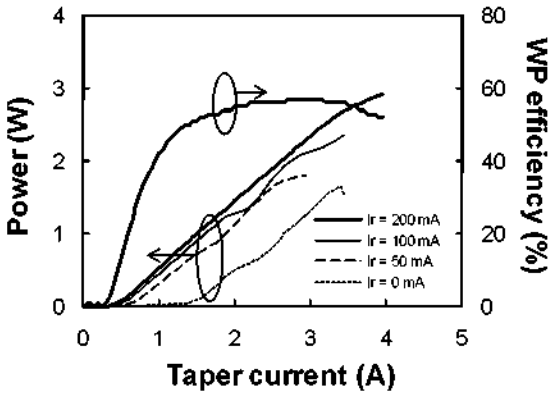

Figure 10: power characteristics
(4 mm laser, 4° angle, 10°C CW)

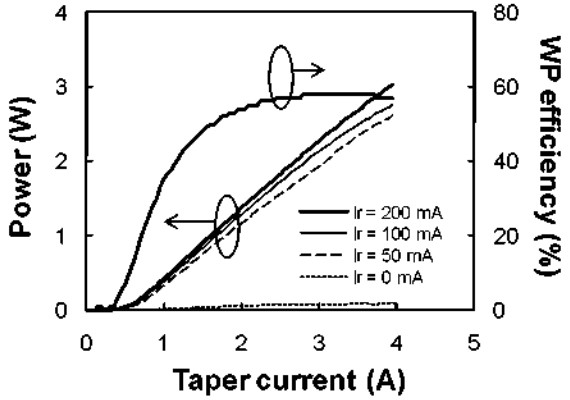

Figure 11: power characteristics
(4 mm laser, 6° angle, 10°C CW)

Note :
On the 6° laser, and under lower I_{taper} = 2.5 A, the power moves from 70 mW (I_{ridge} = 0 mA) to around 1.68 W (I_{ridge} = 80 mA), so that ME = 20 W/A. This value will be useful for comparisons with operation in the dynamic regime in section V.

Tapered lasers with 3 mm length

The power characteristics of the 4° lasers are shown in Figure 12 for several values of I_{ridge}. The laser delivers up to 1.6 W power at 10°C CW (I_{ridge} = 300 mA, I_{taper} = 2A). When I_{ridge} = 0 mA, lasing occurs when I_{taper} is larger than 1.5 A. For (I_{ridge} = 50 mA, I_{taper} = 1.5 A), the power is of 0.92 W, and for (I_{ridge} = 0 mA, I_{taper} = 1.5 A) the power is of 40 mW so that the modulation efficiency is of :

$$ME = \frac{\Delta P_{Opt}}{\Delta I_{ridge}} = \frac{0.92 - 0.04}{0.05} = 18\ W/A \qquad \text{(EQ 6)}$$

The power characteristics of the 6° lasers are shown in Figure 13 for several values of I_{ridge}. The laser delivers up to 1.5 W power at 10°C CW (I_{ridge} = 300 mA, I_{taper} = 2A). When I_{ridge} = 0 mA, lasing occurs when I_{taper} is larger than 1.0 A. For (I_{ridge} = 50 mA, I_{taper} = 1.0 A), the power is of 0.45 W, and for (I_{ridge} = 0 mA, I_{taper} = 1.0 A) the power is of 50 mW so that the modulation efficiency is of :

$$ME = \frac{\Delta P_{Opt}}{\Delta I_{ridge}} = \frac{0.45 - 0.05}{0.05} = 8\ W/A \qquad \text{(EQ 7)}$$

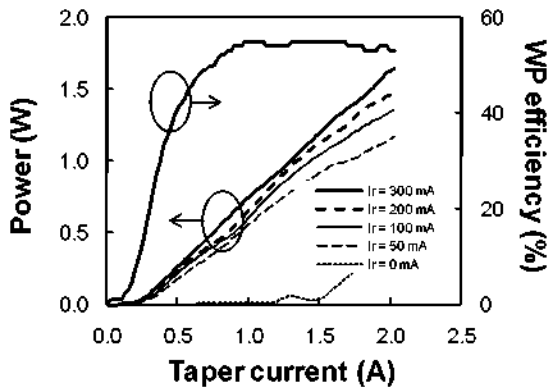

Figure 12: power characteristics
(3 mm laser, 4° angle, 10°C CW)

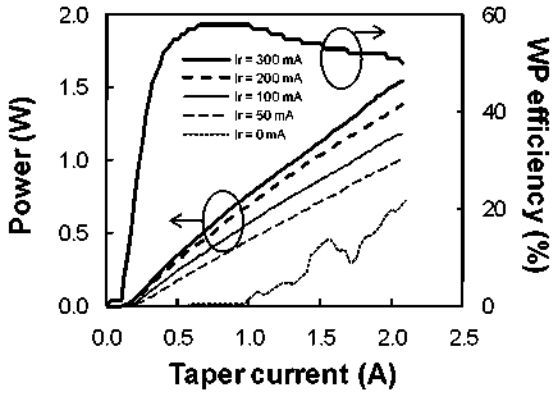

Figure 13: power characteristics
(4 mm laser, 6° angle, 10°C CW)

On both 3 mm lasers, the maximum power does not exceed 1.6 W, which is almost half of the 3 W maximum power on both 4 mm lasers. This difference is mainly explained by thermal effects caused by the smaller surface of the 3 mm lasers, and by thicker submounts on the 3 mm lasers.

Note :
On the 4° laser, and under lower I_{taper} = 1.1 A, the power moves from 10 mW (I_r = 0 mA) to around 0.63 W (I_r = 50 mA), so that ME = 13 W/A. This value will be useful for comparisons with operation in the dynamic regime in section V.

IV- BEAM PROPERTIES MEASURED IN THE STATIC REGIME

Tapered lasers with 4 mm length

First, we present the beam properties of the 4° laser (Figures 14 and 15). We have measured the near-field of the laser with a CCD camera, which shows a main central lobe (8.5 µm FWHM), and several lower sidelobes (41 µm at $1/e^2$), which come from the combined effects of the non-uniform distribution of the carriers and temperature inside the tapered section of the laser [6]. Based on these measurements, we have calculated the M^2 beam propagation ratio at $1/e^2$, according to the following formula:

$$M^2_{1/e^2} = \frac{\pi}{4\lambda} w_{1/e^2} \theta_{1/e^2} = 3.1 \qquad \text{(EQ 7)}$$

Second, we have performed the same measurements on the 6° laser (Figures 16 and 17), finding a similar M^2 of 3.2 at $1/e^2$. However, the beam widths, divergence angles and astigmatism from the 6° laser are different from those of the 4° laser, respectively (Table 2).

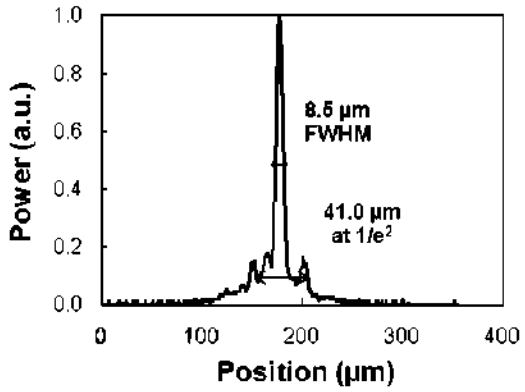

Figure 14: near-field at waist at
(4 mm laser, 4° angle, 10°C CW)
I_r = 200 mA, I_t = 3.5 A, P_{opt} = 2.7 W

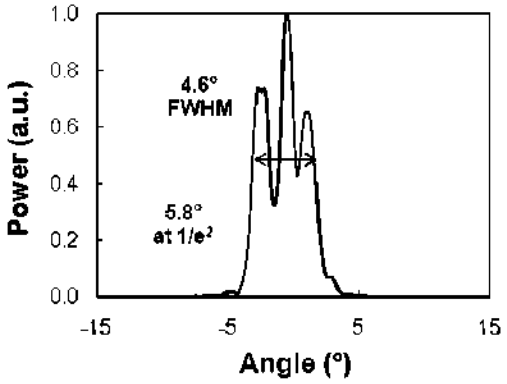

Figure 15: far-field
(4 mm laser, 4° angle, 10°C CW)
I_r = 200 mA, I_t = 3.5 A, P_{opt} = 2.7 W

These comparisons indicate the lower thermal effects on the 6° laser, which has a larger surface, and that the 6° angle seems to be in better adequation with the propagation of the beam inside the taper, whereas the 4° angle may be too narrow for the beam to freely expand inside the laser [8, 9].

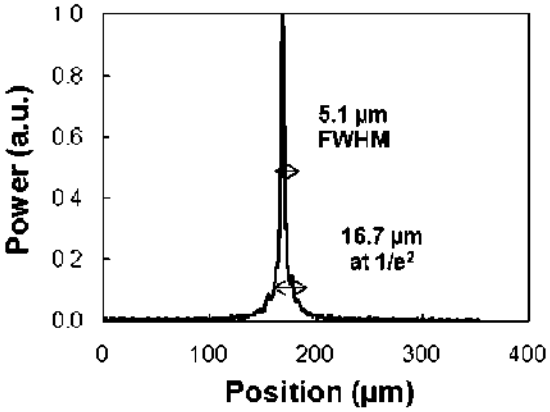

Figure 16: near-field at waist
(4 mm laser, 6° angle, 10°C CW)
I_r = 200 mA, I_t = 3.5 A, P_{opt} = 2.7 W

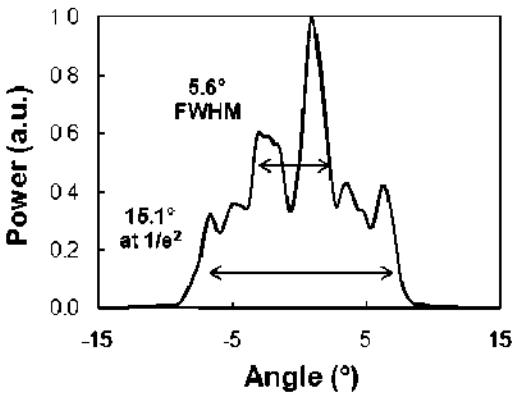

Figure 17: far-field
(4 mm laser, 6° angle, 10°C CW)
I_r = 200 mA, I_t = 3.5 A, P_{opt} = 2.7 W

Table 2: Beam properties of the 4 mm lasers (I_r = 200 mA, I_t = 3.5 A)

Taper angle (°)	Power (W)	w FWHM (µm)	w at 1/e² (µm)	$\theta_{//}$ FWHM (°)	$\theta_{//}$ at 1/e² (°)	M^2 at 1/e²	Astigmatism (µm)
4	2.7	8.5	41.0	4.6	5.8	3.1	1400
6	2.7	5.1	16.7	5.6	15.1	3.2	1020

Tapered lasers with 3 mm length

First, we present the beam properties of the 4° laser (Figures 18 and 19). The near-field shows a main central lobe (7 µm FWHM, 15 µm at 1/e²). The far-field has a divergence of 4.5° FWHM and 8.7° at 1/e². Based on these measurements and on (EQ 7), we find a good M^2 beam propagation ratio of 1.8.

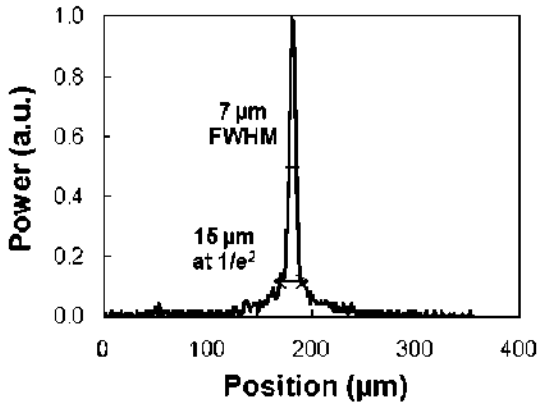

Figure 18: near-field at waist
(3 mm laser, 4° angle, 10°C CW)
I_r = 200 mA, I_t = 1.5 A, P_{opt} = 1.1 W

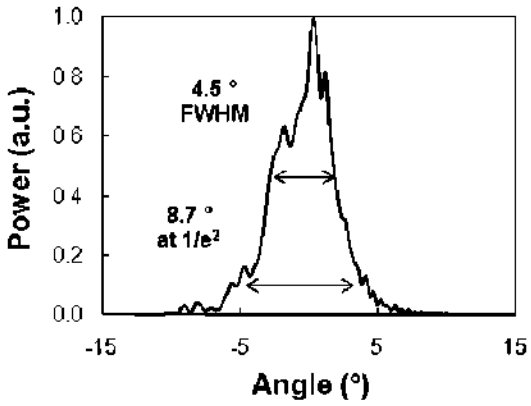

Figure 19: far-field
(3 mm laser, 4° angle, 10°C CW)
I_r = 200 mA, I_t = 1.5 A, P_{opt} = 1.1 W

On the 6° lasers (Figures 20 and 21), we find a narrower near-field (5.3 µm FWHM, 10.9 µm at 1/e²), and a broader far-field divergence (6.2° FWHM, 14.7° at 1/e²). The 6° lasers seem to have a narrower beam waist (Table 3) because of their reduced thermal load, and because of the better matching of the taper angle with the propagation of the beam inside the laser [9].

Table 3: Beam properties of the 3 mm lasers (I_r = 200 mA, I_t = 1.5 A)

Taper angle (°)	Power (W)	w FWHM (µm)	w at 1/e² (µm)	$\theta_{//}$ FWHM (°)	$\theta_{//}$ at 1/e² (°)	M^2 at 1/e²	Astigmatism (µm)
4	1.1	7.0	15.0	4.5	8.7	1.8	880
6	1.0	5.3	10.9	6.2	14.7	2.1	710

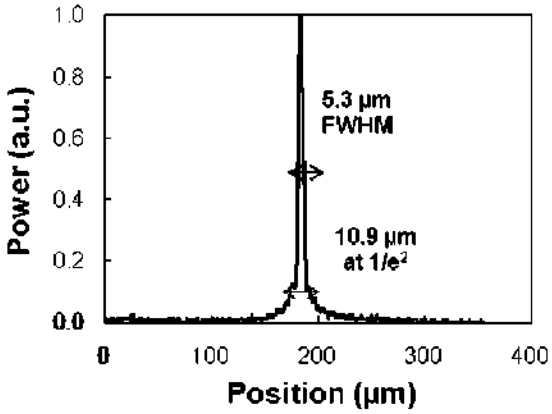

Figure 20: near-field at waist
(3 mm laser, 6° angle, 10°C CW)
I_r = 200 mA, I_t = 1.5 A, P_{opt} = 1.0 W

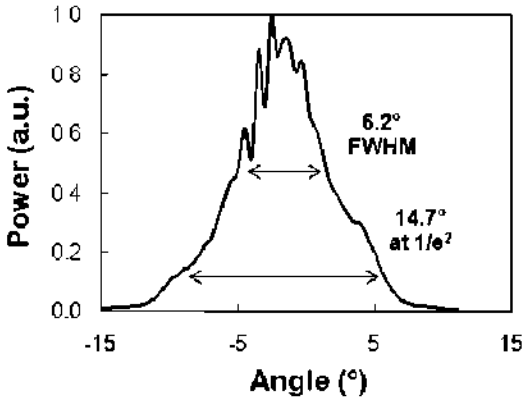

Figure 21: far-field
(3 mm laser, 6° angle, 10°C CW)
I_r = 200 mA, I_t = 1.5 A, P_{opt} = 1.0 W

V- TWO-SECTION TAPERED LASERS MEASURED IN THE DYNAMIC REGIME

In section II, we have studied two-sections tapered lasers theoretically, and in section III, we have obtained high modulation efficiencies of up to 50 W/A experimentally. In this section, we use the two-section tapered lasers for digital transmissions.

6° tapered lasers with 4 mm length

In this experiment (Figure 22), the two-section laser is biased with two current sources, including one DC source of 2.5 A connected to the tapered section of the laser, and one signal source connected to the ridge section. The current on the ridge is modulated with NRZ signals between 22 mA and 106 mA. The impedance matching between the current driver and the ridge is made through a 50 Ω resistor.

Under these conditions, we have obtained a clear eye diagram at 700 Mbps (Figure 23). The output optical power is modulated between 22 mW and 1.68 W, which corresponds to an optical modulation amplitude of 1.66 W, together with an extinction ratio of 19 dB. The corresponding modulation efficiency is of

$$ME = \frac{\Delta P_{Opt}}{\Delta I_{ridge}} = \frac{1.68 - 0.02}{0.106 - 0.022} = 19\ W/A \qquad \text{(EQ 8)}$$

Note:
The 19 W/A value of the modulation efficiency is similar to that of the same laser operated in the static regime (see section III).

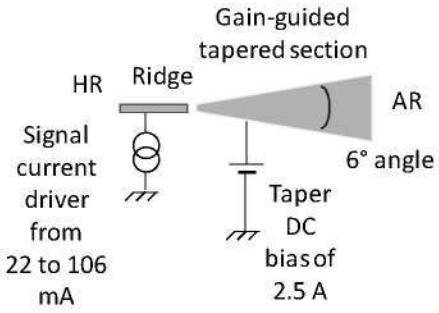

Figure 22: modulation of 4 mm laser

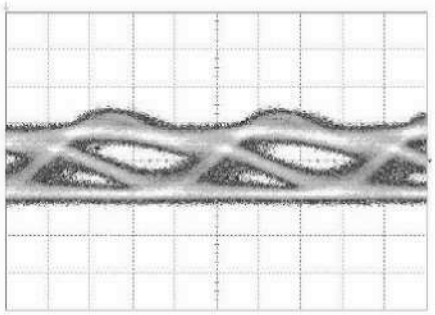

Figure 23: open eye diagram at 700 Mbps
(360 ps per division)

4° tapered lasers with 3 mm length

In this experiment (Figure 24), the two-section laser is biased with two current sources, including one DC source of 1.1 A connected to the tapered section of the laser, and one signal source connected to the ridge section. The current on the ridge is modulated with NRZ signals between 8 mA and 48 mA. The impedance matching between the current driver and the ridge is made through a 50 Ω resistor.

Under these conditions, we have obtained a clear eye diagram at 1 Gbps (Figure 25). The output optical power is modulated between 50 mW and 580 mW, which corresponds to an optical modulation amplitude of 0.53 W, together with an extinction ratio of 11 dB. The corresponding modulation efficiency is of

$$ME = \frac{\Delta P_{Opt}}{\Delta I_{ridge}} = \frac{0.58 - 0.05}{0.048 - 0.08} = 13\ W/A \qquad \text{(EQ 9)}$$

Note:
The 13 W/A value of the modulation efficiency is similar to that of the same laser operated in the static regime (see section III).

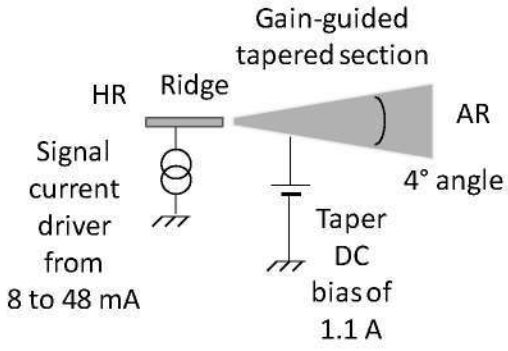

Figure 24: modulation of 3 mm laser

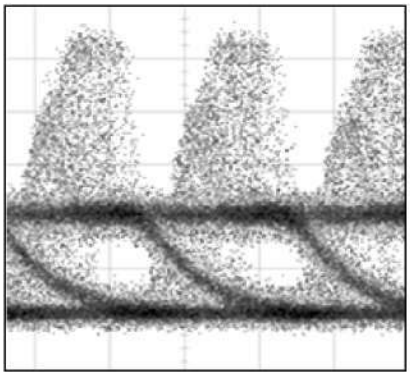

Figure 25: open eye diagram at 1 Gbps
(~ 500 ps per division)

CONCLUSIONS

On an Al-free active region structure, we have obtained low losses of 0.9 cm^{-1} and a high internal quantum efficiency of 98%. Based on this structure, we have simulated two-sections tapered lasers with a high modulation efficiency. Two types of lasers were realized, with either 4 mm length or 3 mm length, respectively. On the 4 mm length lasers, in the static regime, we have obtained a very high modulation efficiency of 50 W/A, together with a high power of 3 W, and a high maximum wall-plug efficiency of 58%. On the 4 mm laser in the dynamic regime, we have obtained a high optical modulation amplitude of 1.6 W, together with a high extinction ratio of 19 dB, and a high modulation efficiency of 19 W/A, and an open eye diagram at 700 Mbps. On the 3 mm laser, in the dynamic regime, we have obtained a high optical modulated amplitude of 530 mW, together with a high modulation efficiency of 13 W/A, a high extinction ratio of 11 dB, and an open eye diagram at 1 Gbps. The latter device will be included into a free-space optical communications module for building-to building communications.

ACKNOWLEDGEMENTS

The authors gratefully acknowledge the support of the European Commission through the IST project n°2005-035266, WWW.BRIGHTER.EU (www.ist-brighter.eu). The authors would like also to thank C. Dernazaretian and P.A. Bernard for excellent technical assistance.

REFERENCES

[1] Lichtenstein, N., Manz Y., Mauron, P., Fily, A., Arlt, S., Thies, A., Schmidt, B., Müller, J., Pawlik, S., Sverdlov, B. and Harder, C., "Singlemode Emitter Array Laser Bars for High-Brightness Applications," Proc. ISLC, Paper ThA6, 45-46 (2004)

[2] Petrescu-Prahova, I.B., Modak, P., Goutain, E., Bambrick, D., Silan, D., Riordan, J., Moritz, T., and Marsh, J.H., "253 mW/μm Maximum Power Density from 9xx nm Epitaxial Laser Structures with d/Γ Greater than 1 μm," Proc. ISLC, Paper WA3, 135-136 (2008)

[3] Sumpf, B., Hasler, K.H., Adamiec, P., Bugge, F., Dittmar, F., Fricke, J., Wenzel, H., Zorn, M., Erbert, G., and Trankle, G., "High brightness quantum well tapered lasers (*Invited Paper*)," IEEE Journal of Selected Topics in Quantum Electronics, 15(3), 1009-1020 (2009)

[4] Michel, N., Odriozola, H., Kwok, C. H., Ruiz, M., Calligaro, M., Lecomte, M., Parillaud, O., Krakowski, M., Xia, M., Penty, R.V., White, I.H., Tijero, J.M.G,. and Esquivias, I., "High Modulation Efficiency and High Power 1060 nm Tapered Lasers with Separate Contacts," Electronics Letters, 45(2), 103-104 (2009)

[5] Dross, F., Van Dijk, F., Parillaud, O., Vinter, B., and Vodjdani, N., "Single-Transverse-Mode InGaAsP–InP Edge-Emitting Bipolar Cascade Laser," IEEE Journal of Quantum Electronics, 41(11), 1356-1360 (2005)

[6] Kwok, C.H., Xia, M., Penty, R.V., White, I.H., Michel, N., Ruiz, M., Krakowski, M., Calligaro, M., Lecomte, M., Parillaud, O., Odriozola, H., Tijero, J.M.G. and Esquivias, I., "Two-Electrode High Power Tapered Laser with up to 40.5 W/A Static Modulation Efficiency and 700 Mb/s Direct Modulation Capability," Proc OFC, Paper OThT8 (2009)

[7] Borruel, L., Sujecki, S., Moreno, P., Wykes, J., Krakowski, M., Sumpf, B., Sewell, P., Auzanneau, S.C., Wenzel, H., Rodríguez, D., Benson, T.M., and Larkins, E.C. "Quasi-3-D Simulation of High-Brightness Tapered Lasers," IEEE Journal of Quantum Electronics, 40(5), 463-472 (2004)

[8] Odriozola, H., Tijero, J.M.G., Esquivias, I., Borruel, L., Martin-Minguez, A., Michel, N., Calligaro, M., Lecomte, M., Parillaud, O., Ruiz, M. and Krakowski, M. "Design of 1060 nm Tapered Lasers with Separate Contacts," Optical and Quantum Electronics, 40(14), 1123 (2009)

[9] Esquivias, I., Odriozola, H., Tijero, J.M.G., Borruel, L., Sujecki, S. and Larkins, E.C. "Operating Principles and Performance Limits of High Brightness Tapered Lasers," www.bright-eu.org (2005)